Temperature-Switchable Control of Ligand Display on Adlayers of Mixed Poly(lysine)- g -(PEO) and Poly(lysine)- g -(ligand-modified poly- N -isopropylacrylamide)

F. Dalier, F. Eghiaian, S. Scheuring, E. Marie, C. Tribet

Temperature-switchable control of ligand display on adlayers of mixed poly(lysine)-g-(PEO) and poly(lysine)-g-(ligand-modified poly-N-isopropylacrylamide).

F. Dalier,[a] F. Eghiaian,[b] S. Scheuring,[b] E. Marie,[a] and C. Tribet*,[a].

[a] Ecole Normale Supérieure-PSL Research University, Dpt Chimie, Sorbonne Universités - UPMC Univ. Paris 06, CNRS UMR 8640, 24 rue Lhomond, 75005 Paris, France. E-mail : christophe.tribet@ens.fr

[b] U1006 INSERM, Aix-Marseille Université, Parc Scientifique et Technologique de Luminy, 163 av. de Luminy, 13009 Marseille, France.).

ABSTRACT

Adlayers of poly(lysine)-g-PEG comblike copolymer are extensively used to prepare cell-repellant and protein-repellent surfaces by a straightforward coulomb-driven adsorption that is compatible with diverse substrates (glass, petri-dish, etc). To endow surfaces with functional properties, namely controlled ligand-protein binding, comb-like poly(lysine) derivatives were used to deposit temperature-responsive poly(NIPAM) macrografts mixed with PEG ones on glass surfaces. Simple surface immersion in mixed solutions of biotin-modified poly(lysine)-g-poly(N-isopropyl acrylamide) and poly(lysine)-g-poly(ethylene oxide) yielded robust adlayers whose composition reflected the ratio between the two polymers in solution. We show by fluorescence imaging, and comparison with repellent 100% PEGylated patterns, that specific binding of model avidin:particle conjugates (diameters of ca. 10 nm or 200 nm) was controlled by temperature switch. The biotin ligand was displayed and accessible at low T, or hidden at T > LCST. Topography and mechanical mapping measurements by AFM confirmed the swelling/collapse status of PNIPAM macrografts in the adlayer at low/high T respectively. Temperature-responsive comb-like PLL derivative that can spontaneously cover anionic interfaces is a promising platform enabling good control on the deposition and accessibility of biofunctional groups on various solid surfaces.

INTRODUCTION

   Spatiotemporal control of surface properties is highly in demand for a diversity of approaches that aim to endow layers of polymers and surface-attached polymer brushes with controlled association to proteins, biocolloids, cells, and recently via in situ stimuli-responsiveness.[1,2] For instance, thick swellable polymer patterns have been designed to control surface accessibility.[3] Thinner polymer brushes are used in diverse applications including assemblies of nano or microparticles,[4] biosensors, [5,6,7], control of bacterial adhesion [8] or cell spreading,[9] controlled flow in microfluidic and separative techniques.[10,11,12] A common design strategy to prepare responsive polymer layers relies on transitions from poor to good solvent conditions, which is conveniently based on conformational transition at the lower critical solution temperature (LCST) in water. LCST properties have been extensively studied in aqueous solutions and in polymer layers (e.g. with derivatives of poly-N-isopropylacrylamide, PNIPAM). The critical challenge for surface-targeted applications is now to achieve specificity i.e. to tailor polymer layers undergoing phase transitions in 2D that provide on demand switchable accessibility of a particular ligand of interest. Reaching this goal is demanding to chemists, as it depends on controlling many key parameters on surfaces, including grafting density and length of polymer chains, distribution of comonomers in copolymer and/or growth of chains having different chemical natures.[13,14,15 and refs therein] Successful proofs of concept have been established based on highly controlled surface polymer chemistry, or deposition of SAM on gold layers (see discussion section for details). But the need for specialized chemistry limits the broadening of such approaches and their wide adoption by biologists. In this context, it is important to develop more versatile coating systems affording robust control and facile modulation, by non-experts, of surface layer composition, and adjustable responsiveness to stimuli.

We propose a polymer architecture to control both the surface-display of ligands, and the ligand density in mixed polymer layers. We relied on spontaneous adsorption of preformed cationic poly(lysine) copolymers, whose advantages are i) to be effective on diverse anionic surfaces,[16, 17] ii) to enable co-adsorption of different polymers and patterning from simple bath application(s), and iii) to alleviate a need for expertise or technical skills, i.e. to be straightforward to use by non specialists. Coating of surfaces by poly(lysine) modified with poly(ethyleneglycol) (PEG macrografts) has been implemented on a variety of surfaces (glass, polystyrene, PDMS) aiming to form protein-repellent or cell-repellent hydrophilic layers [18],[19]. We studied here as a proof of principle, whether PNIPAM-grafted poly(lysine) enables to deposit T-responsive strands on glass, with a tunable surface density (in mixed layers with PEG), and preserves the response to temperature in the adsorbed layers (Scheme 1). Specific vs non-specific binding of avidin-bearing particles, degree of swelling, and rigidity of the patterns were studied by epifluorescence and AFM.

MATERIALS AND METHODS

All chemicals were purchased from Sigma-Aldrich, except diethylether (VWR), sodium tetraborate decahydrate (Fluka), and end-functional polyethyleneglycol (PEG-NHCO-C_2H_4-CONHS, MW 2000 Dalton, RAPP Polymer). Fluorescent probes, Neutravidin-conjugated yellow-green FluoSpheres and QDot 565 Strepavidin-conjugate, were purchased from LifeTechnologies. Azobisisobutyronitrile was recrystalized in methanol, and diethylether was dried on molecular sieves (4 Å) before use. Deionized water was produced by MilliQ, Direct-Q 5 instrument (Millipore).

^{1}H-NMR spectra were recorded at 20 °C on a Bruker Topspin spectrometer (300 MHz). Chemical shifts (δ) are reported in parts per million (ppm) relative to a residual proton peak of the solvent, δ = 2.50 for DMSO and δ = 4.79 for D$_2$O. Multiplicities are reported as: s (singlet), d (doublet), t (triplet), q (quartet), dd (doublet of doublets), dt (doublet of triplets) or m (multiplet). The number of protons (n) for a given resonance is indicated as "n H", and is based on spectral integration values.

Molecular weight and polydispersity of polymers were determined by Size Exclusion Chromatography in DMF at 24 °C, elution through three Viscotek columns (CLM1014/CLM1012/CLM1011, 0.7 mL.min^{-1}) with refractive index detection (Viscotek dectector). Calibration was performed with PS standards kit (Viscotek, 1050 - 64500 Da).

Polymer Synthesis

The synthesis of PLL derivatives comprised two main steps. First, macrografts (e.g. poly(*N*-isopropylacrylamide-co-Biotinacrylamide)) were prepared from a parent poly(*N*-acryloyl succimide) chain by grafting amines, in controlled redox conditions, preserving the thiol end group (Scheme 2a, where x represents the molar fraction of Biotin and w is the molecular weight in g/mol). Second, the end-reactive macrografts were coupled on poly(lysine) to obtain PLL-g-P(NIPAM-co-Biotin$_x$)$_{y,w}$ (where y is the mol% of lysine groups coupled to poly(NIPAM-co-Biotin)).

Synthesis of poly(N-AcryloxySuccinimide) parent chain

Monomer (NAS) was synthesized as follows, a few days prior to its RAFT polymerization. *N*-Hydroxysuccinimide (5.0 g, 0.043 mol) and triethylamine (7.3 mL, 0.050 mol) were dissolved in chloroform (65 mL) at 0 °C. N-acryloylchloride (3.9 mL, 0.047 mol) was added dropwise and

the mix was kept under gentle stirring for 30 minutes at 0 °C. The reaction mixture was washed twice with 30 mL saturated NaCl solution, dried over magnesium sulfate, and concentrated by evaporation yielding viscous oil. Ethyl acetate/pentane (7 mL, 1:3 v/v) was added to the oil at 0 °C to induce NAS crystallization. After filtration and drying under vacuum, the product was obtained as a white solid (5.2 g, 71 %).. δ (^{1}H-RMN, DMSO-d_6) : 2.84 (s, 4H), 6.35 (dd, J = 10.3, 1.2 Hz, 1H), 6.52 (dd, J = 18.1, 10.4 Hz ,1H), 6.67 (dd, J = 17.2, 1.3 Hz, 1H)

NAS (3 g, 18 mmol), AIBN (6 mg, 36 µmol) and 2-(Dodecylthiocarbonothioylthio)-2-methylpropanoic acid (132 mg, 0.36 mmol) were placed into a Schlenk flask and dissolved in anhydrous DMF (6 mL). The solution was degazed by four freeze-pump-thaw cycles, and heated to 85 °C under Argon atmosphere. Aliquots were regularly withdrawn from the reaction medium and analyzed by ^{1}H-NMR (DMSO-d_6) to determine monomer conversion by comparing the relative integral areas of the methyne backbone protons (1.71-2.24 ppm, 2H) to the monomer vinyl proton (6.35 ppm, 1H). Degree of polymerization (DPn) and polydispersity (Ip) were determined by SEC analyses in DMF (cf data in SI figures S1, S2, S3). The chain growth showed an induction period (~50 min) that has already been reported in RAFT polymerization of acrylamides.[20], [21] It was followed by a pseudo-first-order regime characteristic of controlled polymerization (Figure S1 in SI). Polymerization was stopped by freezing the flask in liquid nitrogen after 2h reaction, at ca. 80% conversion. The polymer was precipitated twice in dried diethylether, and dried under vacuum, yielding poly(NAS) as a yellow powder (1.5 g, 51 %).

Synthesis of NHS-PNIPAM derivatives

Freshly synthesized poly(NAS) (100 mg, 0.013 mmol of monomers) and tributylphosphine (0.1 mL) were dissolved in anhydrous DMSO (1.5 mL). To obtain biotin-modified chains,

5mol% of Biotin-NH$_2$ (relative mol% to NAS, scheme 2a-b) was added and the reaction bath was heated up to 40 °C for 2 hours, under Argon, before an excess of isopropylamine (0.12 mL, 1.5 mmol) was added. The addition of biotin was skipped to form pure PNIPAM chains. After two more hours at 40 °C, the polymer was precipitated twice into dried diethylether. The dried polymer, either with or without biotin, contained a thiol end group. 100mg of this dried polymer was dissolved in anhydrous DMSO (2 mL), with 4-maleimidobutyric acid *N*-hydroxysuccinimide ester (2 equiv. relative to thiols) and tributylphosphine (catalytic amount), and kept at room temperature for 6 h under argon atmosphere. The product was precipitated twice into diethylether, and dried under vacuum.

grafting of NHS-PNIPAM copolymers on PLL

Poly(lysine (PLL•HBr, 20 mg, 95 µmol from Sigma-Aldrich) with an average molecular weight of 20 kDa was dissolved in 1 mL of 50mM sodium tetraborate buffer pH 8.5 in water. Aliquot of the NHS-terminated macrograft was added at a final chain:lysine molar ratio of 35 mol%, and the solution was kept at room T overnight, then dialysed (MW cut-off 3.5 kDa) against MilliQ water for one day (three renewal of the bath), and lyophilised. To estimate the degree of grafting of PLL amine groups, the peak areas from unmodified lysine (-CH-(CH$_2$)$_3$-CH$_2$-NH$_3$) and modified ones (-CH-(CH$_2$)$_3$-CH$_2$-NH-CO-) were compared. The PLL grafted with biotin-containing macrografts yielded a degree of modification of lysine of 10 ± 2 mol% ; 20 ± 2 mol% grafting was determined for the polymer coupled with NSH-PNIPAM (no biotin).

PLL-g-(PNIPAM6000)$_{0.20}$, δ (RMN-^{1}H, D$_2$O) : 0.95-1.23 (s, -CH$_2$-CH(CO-NH-CH-(CH$_3$)2)-, 163H), 1.24-2.20 (m, -CH-(CH$_2$)$_3$-CH$_2$-NH$_3$, -CH$_2$-CH(CO-NH-CH-(CH$_3$)$_2$, 93H), 2.87-2.98 (s, -

CH-(CH$_2$)$_3$-CH$_2$-NH$_3$, 1.6H), 3.05-3.17 (s, -CH-(CH$_2$)$_3$-CH$_2$-NH-CO-, 0.4H), 3.75-3.96 (s, -CH$_2$-CH(CO-NH-CH-(CH$_3$)$_2$, 27H), 4.17-4.32 (s, -CH-(CH$_2$)$_3$-CH$_2$-NH$_3$, 1H),

PLL-g-P(NIPAM6000-co-Biotin$_{0.05}$)$_{0.10}$, δ (RMN-^{1}H, D$_2$O) : 0.92-1.22 (s, -CH$_2$-CH(CO-NH-CH-(CH$_3$)$_2$)-, 21H), 1.26-2.29 (m, -CH-(CH$_2$)$_3$-CH$_2$-NH$_3$, -CH$_2$-CH(CO-NH-CH-(CH$_3$)$_2$, 20H), 2.89-3.00 (s, -CH-(CH$_2$)$_3$-CH$_2$-NH$_3$, 1.8H), 3.24-3.31 (s, -CH-(CH$_2$)$_3$-CH$_2$-NH-CO-, 0.7H), 3.73-3.96 (s, -CH$_2$-CH(CO-NH-CH-(CH$_3$)$_2$, 4.1H), 4.16-4.31 (s, -CH-(CH$_2$)$_3$-CH$_2$-NH$_3$, 1H), 4.35-4.42 (proton HA related to the Biotin, 0.2H), 4.53-4.61 (proton HB related to the Biotin, 0.2H)

On the other hand, two additional PLL derivatives were prepared:

PLL-g-(PEG2000)$_{0.4}$, noted as PLL-g-PEG below, was prepared similarly by coupling 2 kDa NHS-PEG onto PLL yielding a degree of grafting of 42mol% (δ (RMN-^{1}H, D$_2$O) : 1.15-1.81 (m, -CH-(CH$_2$)$_3$-CH$_2$-NH$_3$, 6H), 2.82-2.97 (s, -CH-(CH$_2$)$_3$-CH$_2$-NH$_3$, 1.1H), 3.03-3.17 (s, -CH-(CH$_2$)$_3$-CH$_2$-NH-CO-, 0.8H), 3.23-3.35 (s, -O-CH$_2$-CH$_2$-O-CH$_3$, 1.3H), 3.55-3.90 (m, -O-CH$_2$-CH$_2$-O-CH$_3$, 67H), 4.13-4.33 (s, -CH-(CH$_2$)$_3$-CH$_2$-NH$_3$, 1H)

Finally, Alexa-labelled PLL-g-P(NIPAM), quoted AlexaPLL-g-PNIPAM, was synthesized to get a fluorescent reporter of adsorption. Alexa Fluor® 532 NHS Ester (Life Technologies) was dissolved in DMSO (1 mg/mL). PLL-g-(PNIPAM6000)$_{0.20}$ (20 mg) was dissolved in 0.4 mL of 50 mM sodium tetraborate buffer pH 8.5 and an aliquot of the DMSO solution of Alexa NHS Ester (85 µL) was added into aqueous solution. The mixture was stirred for 4 h at room temperature in the dark, prior to dialysis (SpectraPore membrane, MWCO 3.5 kDa) against MilliQ water for one day, and lyophilization yielding a fluorescent powder.

Coating of glass coverslips with PLL derivatives

Glass coverslips (from Bioptechs, catalog number: 130119-5) with a diameter of 40 mm were washed with technical ethanol, sonicated for 45 minutes in a solution of sodium hydroxide (1 mol.L^{-1}), and rinsed with MilliQ water. A solution of PLL derivatives in MilliQ water (either PLL-g-PEG, or PLL-g-PNIPAM containing or not biotin or AlexaFluor) at a total polymer concentration of 1 mg/mL was deposited on the top of coverslips, that were kept at room temperature for 1 hour. The coated surfaces were rinsed with MilliQ water, and stored at 4 °C (in water for storage time < 2 days, or after drying under flushing nitrogen for longer storage times).

To prepare surface patterns with alternating PLL-g-PEG and PLL-g-PNIPAM-containing stripes, a chromium synthetic quartz photo-mask (Toppan, Product type: 5" QZ M1X, cleaned with technical ethanol and then exposed to deep UV light for 5 minutes) was placed on an evenly pre-coated coverslip (e.g. with PLL-g-PNIPAM or PLL-g-PEG), and exposed for 15 minutes to deep UV (UV Ozone cleaner from BioForce Nanosciences) in order to etch 6 μm-large stripes separated by UV-protected gaps of either 25μm or 40μm, Scheme 3). Typically the mask:coverslip sandwich was stacked by a 7 μL drop of water deposited on the mask (this volume has to be adapted to the size of surfaces). After etching, the coverslip was rinsed with MilliQ water, and a 1 mg/mL solution of PLL derivatives in milliQ water was deposited on the surface and incubated for 1 hour (either PLL-g-PEG, or a mixed PLL-g-PNIPAM:PLL-g-PEG solution, see Table 1). Finally, the glass were rinsed with water and stored at 4°C. The compositions of solutions used to deposit PLL derivatives on stripes are summarized in Table 1.

Table 1. Short names of sample coverslips and composition of solutions incubated on stripes.

Short name	Large stripes[a]	Thin stripes[b]

		PNIPAM	PNIPAMcoBiotin	PEG
$S_{PEG/NIPAbiot}$	PEG	-	1	-
$S_{PEG/NIPAbiot:PEG 3:1}$	PEG	-	0.75	0.25
$S_{PEG/NIPAbiot:PEG 1:1}$	PEG	-	0.5	0.5
$S_{PEG/NIPA}$	PEG	1	-	-
$S_{PEG/NIPA:PEG 3:1}$	PEG	0.75	-	0.25
$S_{PEG/NIPA:PEG 1:1}$	PEG	0.5	-	0.5
$S_{NIPA/glass}$	PNIPAM	-	-	-

[a] concentration of the coating polymer solutions were 1 mg.mL^{-1} in water. [b] columns show the concentration (mg.mL^{-1}) of each polymer in the mixed solution used to coat the stripe (zero if not specified). "PEG","PNIPAM", and "PNIPAMcoBiotin" meant for PLL-g-(PEG2000)$_{0.4}$, PLL-g-(PNIPAM6000)$_{0.20}$, and PLL-g-P(NIPAM6000-co-Biotin$_{0.05}$)$_{0.10}$

Capture of particles on patterned surfaces

Patterned coverslips were mounted in a flow cell, which enabled accurate control of the temperature and fluorescence imaging (Focht Chamber System 2, FCS2 from Bioptechs, images taken in a LEICA DMIRE-2 microscope, equipped with a long-focal ×60 objective used in air, ScopeLED Roper Scientific illuminator, and Retina 6000 Q-imaging camera). The chamber was filled with MilliQ water and heated at the desired temperature T_e for 15 minutes. Water present in the chamber was then rapidly ejected by flushing air, and replaced by 100 µL of beads suspension pre-heated at T_e. After incubation for 15min, the chamber was rapidly emptied by flushing air, and rinsed with 2 mL MilliQ water at T_e. Beads suspensions were either Neutravidin-coated FluoSpheres (Polystyrene beads from LifeTechnologies, 0.2 µm diameter at 1 % solids diluted 50 fold in MilliQ water), or Streptavidin-conjugated quantum dots (QDot565 Strepavidin-conjugate from LifeTechnologies, 0.1 µM in MilliQ water). Fluorescence was recorded and the contrast defined as $(I_{stripe}-I_{PEG})/(I_{stripe}+I_{PEG})$, with $I_{stripe/PEG}$ the average intensities measured on 6 stripes. Fluorescence from Alexa-modified polymer layers (Figures 1 and S4 in SI) was low, and measurements were done in open cell, to facilitate handling, with a drop of water deposited on samples. This geometry contributes to enhance the fluctuation of baseline due to reflection of the excitation beam.

AFM measurements

Atomic force microscopy (AFM) was performed on a Bruker Catalyst, using OLYMPUS AC40-TS cantilevers (nominal spring constant 0.09N/m). Polymer-coated glass coverslips were immersed in PBS buffer (137mM NaCl, 2.7 mM KCl,10mM sodium phosphate buffer pH 7.4) that was previously filtered on membranes with a 0.2 µm pore-size. A heated plaque coupled to the AFM X-Y scanner enabled us to modify the sample temperature, which was monitored by immersing a thermocouple under the AFM head. Prior to each AFM measurement, we allowed the sample to equilibrate for 15 minutes. AFM imaging was performed in PeakForce® mode, using a 150-200pN setpoint. In this mode, a piezoelectric actuator oscillates the cantilever with a sinewave in vertical direction and at a 1 kHz frequency, different to the cantilever resonance, thus enabling the acquisition of fast force vs distance curves (FZ curves) during X-Y scan. Informations collected from PeakForce® maps were: sample height, deformation, tip-sample adhesion force, and Young's modulus (as determined by a real-time fitting of force vs distance curves following the assumptions detailed in §3 below).

1) Maps of the tip-sample adhesion, calculated by fitting a baseline to FZ curves and determining the lowest force point in the retraction curves (ie, when the cantilever is pulled away from the sample). Single FZ curves were also performed on the sample at points that were chosen in the PeakForce® topography and adhesion map. The indentation velocity was 2 µm/s and the force setpoint was 200pN.

2) Topographic scan. Due to the application of force onto the surface during topographic scan, the raw data contain the contribution of the local compression of the soft polymer layer. To remove the effect of layer deformation, heights were recalculated at each pixel by extrapolation

of the effective tip position corresponding to zero applied force. To this aim, measurement of the polymer height as obtained by the PeakForce® topography map was added to the deformation maps of the polymer at the force setpoint. The average polymer height was obtained by fitting a gauss function to the height histograms and calculating the difference between polymer-covered and bare glass regions.

3) Estimation of Young's modulus. An effective Young's modulus was determined by fitting the Dejarguin-Müller-Toporov model of adhesive contact to the extension curve (Nominal tip radius: 10nm, Poisson's ratio ν=0.3), following the equation:

$$F - F_{adh} = \frac{4}{3}\frac{E}{1 - \upsilon^2}R^{1/2}\delta^{3/2}$$

with $F - F_{adh}$ the total force from the adhesion peak to the maximum force used for fitting, E the Young's modulus, R the tip radius, δ the indentaion and ν the Poisson ratio. The DMT model was also applied to real-time fitting of force *vs* distance curves in PeakForce® tapping (ESI Figure S9). Prior to fitting curves, it was established that, excluding tip-sample adhesion events, no hysteresis was observed between the extension and retraction force-*vs*-indentation curves (ESI Figure S10).

RESULTS

Surface deposition of PLL derivatives.

PLL-based strategy for coating was inspired by the work from Textor and coll. on robust and efficient surface passivation by adsorbed comblike Poly(lysine)-g-polyethyleneglycol (PLL-g-PEG).[16, 17] The use of functional PLL derivatives that can reversibly bind specific target extends our recent results on reactive, azido-terminated, PEG-g-PLL,[18] to a versatile introduction of amine-containing ligands into responsive adlayers. To this aim, polymer macrografts were

prepared as it follows: a parent homopolymer of N-acryloylsuccinimide obtained by reversible addition-fragmentation chain transfer (number average molecular weight DPn of 50 according to NMR, polydispersity Ip 1.2, NMR and SEC characterizations in SI) was reacted with aliquots of amine-presenting ligand (here a Biotin derivative, cf scheme 2b). Final addition of an excess isopropylamine yielded PNIPAM copolymers containing biotin side groups. The preservation of thiol end group enabled covalent maleimide-thiol coupling to introduce an activated ester end group, and next attachment of the PNIPAM macrografts into PLL (cf material & methods). In the following, "PLL-g-PNIPAM" refers to the copolymer with 20 mol% of the lysine groups of PLL being grafted by PNIPAM strands (no Biotin), and "PLL-g-PNIPAMcoBiotin" to 10 mol% grafting degree of PLL by PNIPAM strands containing 5 mol% of Biotin side groups (ca. 2-3 Biotin per macrograft). PLL-g-PNIPAM was also labelled with 0.5 mol% AlexaFLuor ("AlexaPLL-g-PNIPAM", cf material and methods) affording to characterize the adlayers by fluorescence. Deposition of PLL comblike chains on cleaned glass coverslips was spontaneously obtained from bath application of aqueous solutions of the polymer of interest (always at 1 g/L). To assess composition in the deposited layers, coverslips were first incubated with mixed PLL-g-PEG:AlexaPLL-g-PNIPAM in water (1 g/L total concentration). Surfaces were water-rinsed, and UV-etched to form bare glass stripes used as reference for fluorescence baseline (cf method section). Fluorescence intensities displayed by the pattern of stripes (Fig. 1) varied essentially in proportion to the fraction of Alexa-labelled chains present in the initial mixed coating solution. More accurately, the representation of fluorescence intensity as a function of concentration shows values slightly below the diagonal in Figure 1B, suggesting a slightly preferential competitive adsorption of PLL-g-PEG (shift < 10%, which was of the order of signal fluctuations).

On the other hand, the adsorbed PNIPAM layers were stable over hours-long incubation in milliQ water (no variation of fluorescence) and against high-T/low-T cycling in water (Fig. S4A in SI). Similarly, fluorescence of 100% AlexaPLL-g-PNIPAM stripes did not vary during incubation with a 1 g/L PLL-g-PEG aqueous solution, suggesting the absence of displacement of pre-adsorbed AlexaPLL-g-PNIPAM by later addition of PLL-g-PEG (Fig S4B in SI). Finally, incubation in AlexaPLL-g-PNIPAM of surfaces precoated with PLL-g-PEG showed only a weak increase of intensity compared to stripes coated with 100% AlexaPLL-g-PNIPAM (Fig. S4B in SI). The weak loss of contrast after application (and rinsing out) of a solution of AlexaPLL-g-PNIPAM indicates that PLL-g-PNIPAM did not significantly displace preformed layers of PLL-g-PEG. Altogether these results show that controlled composition of mixed adlayers are achieved, and that these layers are stable to rinsing and further contacts with other grafted PLL copolymers. This stability is not surprising, and is presumably due high repulsion barrier formed by the initially bound chains.[16,17]

Binding of avidin-conjugated beads

To assess the specific binding on biotin-containing layers, glass surfaces were prepared by a similar procedure as above, but using PLL-g-PNIPAMcobiotin. The accessibility of the ligand was revealed by the binding of neutravidin-coated polystyrene beads (FluoSphere, 0.2 μm diameter) or strepavidin-conjugated nanoparticles (Qdot-avidin, 15 nm diameter) on coverslips (fixed in a microchamber equipped with a Peltier temperature controller, cf method section). After 15 minutes incubation with either dispersion of FluoSpheres or Qdots, the chamber was flushed with water to remove unbound particles. As shown in Figure 2 by epifluorescence imaging, surface-bound particles were significantly denser at 25°C than at 45°C on the top of

PLL-g-PNIPAMcoBiotin covered stripes. The base-line signal measured above PLL-g-PEG stripes (used as internal reference, devoid of biotin, and expected to be protein-repellent[16,17,18]) was significantly lower.

At 25°C, binding on PLL-g-PNIPAMcobiotin was high and indicated biotin accessibility. With FluoSpheres, the higher binding, and also higher variation of the density of bound particles upon increasing the temperature was reached on stripes made of 100% PLL-g-PNIPAMcoBiotin (Table 2). The threshold temperature of switching between high and low densities of bound FluoSpheres was estimated to be ca. 30°C (Figure S7 in SI). Stripes coated by mixed PLL-g-NIPAMcobiotin:PLL-g-PEG solutions became rapidly inert upon decreasing the density of biotin, i.e. displayed low, presumably non-specific binding, and absence of temperature-triggered binding below a fraction of 50% NIPAMcobiotin ($S_{PEG/NIPAbiot:PEG\ 1:1}$ in Table 2), indicating that biotin density is also a critical parameter. In each coverslip, the 100% PEGylated stripes were used as an independent internal "blank" (control surface). The regions coated with 100% PLL-g-PEG typically displayed < 5 bound FluoSphere per stripe. An additional reference for non-specific binding was PLL-g-PNIPAM-covered stripes (no biotin). A slight non-specific adsorption of FluoSpheres on the 100% PLL-g-PNIPAM covered regions could be measured ($S_{PEG/NIPA}$ in Table 2). This non-specific binding decreased significantly, by a factor of ca. 2 on mixed PLL-g-PNIPAM:PLL-g-PEG layers ($S_{PEG/NIPA:PEG\ 3:1}$ and $S_{PEG/NIPA:PEG\ 1:1}$). Non-specific adhesion was always significantly below the specific binding observed at 25°C ($S_{PEG/NIPAbiot}$).

Streptavidin-conjugated Qdots cannot be isolated as single particles on fluorescence images, thus quantification of their adsorption was based on the contrast between PLL-g-PNIPAMcobiotin coated stripes and the 100% PLL-g-PEG stripes used as internal reference (cf method, and Table 3). Intensity of Fluorescence on 100% PLL-g-PEG exposed to Qdots was low

but non-zero (see Figures S5-S6 in SI) and did not significantly differ at 25°C and 45°C (Table S2 in SI). Only stripes coated by pure PLL-g-PNIPAMcobiotin, and incubated at 25°C, showed significant contrast compared to PLL-g-PEG, suggesting that specific binding only occurred on the layer containing the denser amount of biotin (for instance, mixed PLL-g-PNIPAMcoBiotin : PLL-g-PEG at 3:1 mol/mol was essentially comparable to pure PLL-g-PEG, i.e. essentially repellent, irrespective of temperature). The specific binding of streptavidin-conjugated Qdots on $S_{PEG/NIPAbiot}$ coverslips was significantly high at 25°C, and low at 45°C (of the order of experimental error). In term of non-specific adhesion of Qdots, PLL-g-PNIPAM layers without biotin compared well with PLL-g-PEG ones (contrast<5% at 25°C, weak non-specific adsorption of Fluorospheres, see SI Fig. S5 and Table 3). Even at 45°C when NIPAM strands are expected to collapse and become hydrophobic, weak contrast was observed compared to 100% PEG-coated regions, irrespective of the presence or absence of Biotin (Fig. 2 and S5). A fluorescence intensity similar to the one of PEGylated stripes suggests that binding onto PLL-g-PNIPAM (at 45°C), but also on PLL-g-PNIPAMcobiotin at 45°C is weak.

Table 2: Number of FluoSpheres counted over a 57 μm segment of PLL-g-NIPAM-coated stripe (average over 351 μm^2) after incubation with Neutravidin-coated FluoSpheres at 25 and 45 °C

T (°C)	$S_{PEG/NIPAbiot}$	$S_{PEG/NIPAbiot:}$ PEG 3:1	$S_{PEG/NIPAbiot:}$ PEG 1:1	$S_{PEG/NIPA}$	$S_{PEG/NIPA:}$ PEG 3:1	$S_{PEG/NIPA:PEG}$ 1:1
25	140 ± 39	60 ± 38	3± 3	31 ± 6	15 ± 3	12 ± 9
45	12 ± 9	12 ± 12	3± 3	27 ± 23	20 ± 8	11 ± 2

Table 3: Fluorescence contrast between NIPAM-coated stripes and PEGylated ones after adsorption of QDs.

T (°C)	$S_{PEG/NIPAbiot}$	$S_{PEG/NIPAbiot:PEG\ 3:1}$	$S_{PEG/NIPA}$	$S_{PEG/NIPA:PEG\ 3:1}$
25	38% ± 3.5%	9 %± 3%	<1%± 4%	5 %± 5%
45	8 %± 3%	5 %± 2.5%	5 %± 3%	0 %± 5%

AFM characterization of PNIPAM layer.

Morphological changes and variation of rigidity of the deposited PNIPAM layers were investigated by in situ AFM [14,22] in PBS buffer, evidencing the transverse shrinkage and stiffening above 33°C. First the change in thickness of the PLL-g-PNIPAM layer was evaluated by recording topographic profiles at increasing temperature across PNIPAM-coated stripes and bare glass ones (on $S_{NIPA:glass}$, Fig. 3a-c). PeakForce QNM, is a force-distance curve-based imaging mode that allows concomitant determination of the elasticity at each sample interaction point,[23,24] and measurement of compression-corrected topography on soft samples. Referred to the average level of bare glass, the average height above PLL-g-PNIPAM layer decreased from 3.6 nm to ~2.2 nm with increasing the temperature from 26°C to 33°C (Fig. 3). Variation of layer thickness by a factor of 1.6 corresponds to usual PNIPAM collapse transition.[25] In addition, AFM images displayed surface roughness with protrusions having submicrometer lateral length scale. These heterogenities in the height (protrusions) were observed at all temperatures, but were relatively flat at low T (+/- 0.5 nm at 26°C) and more prominent at high T (+/- 2-3 nm at 37°C). At high temperature, heterogenities in the height became similar to the average thickness suggesting that bare glass may be accessible at high temperature between these protrusions (see Fig. 3a,c and SI Fig. S8). The lateral size of protrusions ranged from 10 to 80 nm, which is considerably larger than dimension of an isolated PLL-g-PNIPAM chain. It is likely that these heterogeneities correspond to lateral aggregation. Morphological changes at high temperature were accompanied by hardening of the PNIPAM layer (Fig. 3d, apparent Young's modulus increased by one order of magnitude). The predicted influence of the substrate on the Young's modulus was less than 2.2-fold, which was small compared to the observed hardening (~1.5-2

orders of magnitude).[26] Upon cooling the sample back to 25°C, the surface recovered its initial softness, height, and homogeneity, showing the reversibility of the transition. Finally, we scanned surfaces alternating 100% PLL-g-PEG stripes and 100% PLL-g-PNIPAM ones (S$_{PEG/NIPA}$). In this case, the two polymer layers developed similar repulsive interactions with the AFM tip at low temperature (27°C in Fig. 4) and similar height as a smooth profile was obtained. Force-distance curves (cf AFM in methods section) with an adhesive regime were obtained at 36°C above PLL-g-PNIPAM, while PLL-g-PEG stripes remained repulsive on average (with attractive spots appearing, tough exhibiting significantly weaker attraction than above the NIPAM-coated regions). Temperature-triggered switch from repulsive to attractive interaction (and its reversibility upon cooling back to 27°C, Fig. 4) add further evidences for reversible phase transition of NIPAM at ca. 32°C in the adlayer.

DISCUSSION

Tight attachment of polymers on surfaces can be produced by diverse strategies, but preparation of mixed layers with adjustable density of functional moieties is not an obvious task. Two approaches predominate. First, the "grafting from" strategy is based on the growth of polymer chains on substrates that are previously modified with chain-initiators. This method leads to the formation of the densest polymer brushes. However, controlling the growth of two polymer strands of different chemical natures, with a controlled ratio between the two polymers, is hardly accessible to non-specialists. This usually requires deposition of two different intiators on the surface for the sequential polymerizations of the two chain types, that shall not interfere. [27,28] Recent introduction of Y-shaped bifunctional initiator enables robust control on the

initiation of two different polymerizations with 1:1 molar ratio (for instance ATRP/Nitroxide Mediated Radical Polymerization[29], [30], or Ring Opening Polymerization/Nitroxide Mediated Radical Polymerization[31]). Nevertheless, surface composition and properties has to be carefuly assessed because of sensitivity of chain growth to conditions of synthesis. The alternative strategy, "grafting to", involves covalent coupling of preformed chains that are preadsorb as mixed polymer layers . For instance, mixed layers have been obtained on gold by adsorption of thiol or dithiobenzoate terminated polymers, or using silanes, amine, or activated esters on pretreated glass or polystyrene substrates. Manipulation of chains of different chemical natures is however a delicate balance, because low polymer-polymer compatibility can induce phase transition[32],[29],[33] and affects homogeneity of the mixed layers.

Compared to covalent modification of surfaces, coatings by tight adsorption are more amenable to deposition of mixtures of chains. A few reports proves that mixed layers can be obtained from mixed solutions of diblock copolymers containing one anchoring block (e.g. a polycation [34],[35], [36]) and a second block of diverse chemical natures. Comb-like PLL derivatives belong to this class of systems. Up to now, preparations of mixed PLL layers aim to achieve high repellency (e.g. to diminish binding of proteins or cells).[16] In contrast, we reported the possible control of attraction on mixed layers formed by PLL derivatives, once in the case PLL-g-PEG having reactive end-groups[18], and in the case of temperature-triggered aggregation of PLL-g-PNIPAM latex beads [37] The major application of PLL-g-PEG is biocompatible coating, that has been extensively studied and is now included in commercial devices. Mixed functionalized PLL derivatives open accordingly an easier, straightforward route to deposit polymer strands of different natures, with no requirement of expertise in surface chemistry. The advantage of full

repellency provided by PLL-PEG layers is combined here with reversible display of a ligand for controlled specific binding. Reversible control of ligand display on biocompatible substrates should broaden the potential of application of PLL coatings for modification of cell-culture substrates, and in general open new opportunities for mild control of targeting, and temporal control of binding in complex biological fluids.

Interestingly, our results show that above LCST, ligands were not accessible to aviding-coated beads, and presumably trapped in aggregates of polymers (the 80nm wide, 5nm high protrusions detected by AFM). This effect goes in reverse direction compared to reported switches (e.g. tight binding of streptavidin at 45°C and low binding at 25°C on self-assembled monolayers of T-responsive strands [38], high cell binding at high T achieved on thicker layers of pure PNIPAM. [13], [3]) On thick PNIPAM films, it is typically shown that cell adhesion can occur at high T, after spontaneous protein binding due to hydrophobic associations, and that repellency is triggered by swelling at low T.[6], [39] The reverse switch, i.e. from low-T attractive to high-T repulsive properties , can however be obtained in mixed layers containing T-responsive and non-responsive chains. The variation of ligand accessibility in mixed layers is generally based on a marked difference between the extensions of chains that display a ligand, and ligand-free (repellent) chains. Upon stimulation, the position of ligands switch from inside to outside the repellent layer (e.g. become buried at high T when it is attached to PNIPAM strands).[40],[28], [41], [42] Although a similar principle may apply to mixed PLL-g-PEG:PLL-g-PNIPAMcobiotin layers, the maximal contrast of binding was in our case observed on pure PLL-g-PNIPAMcobiotin. Here by design, PNIPAM strands were of similar length as PEG ones, and part of the biotin can be buried in the adlayer because it was distributed randomly in the PNIPAM strands. It was noticed

that surface aggregates were formed above LCST and were highly rigid. In these conditions, possible mechanisms can be proposed to interpret the lack of biotin accessibility at high T. First, it could be that solid-like clusters of chains limit accessibility of the biotin groups trapped inside these clusters, leading in addition to absence of biotin on the surface of clusters (lack of biotin on cluster-water surface is a possible consequence of hydrophobic attraction within the collapsed PNIPAM). Second, it is possible that surface roughness emerging at T> LCST diminishes accessibility due to steric effects : formation of a few nanometer thick rigid protrusions hampers the accessibility to all ligands due to a limited area of contacts between aviding-coated beads and the upper cap of "protrusions". A threshold surface density of ligand is required to bind the beads (which is validated by the rapid loss of specific binding on mixed PEG:PNIPAM-co-biotin layers). Roughness and/or partial burial in PNIPAM clusters are both capable to decrease below this threshold the number of accessible biotin per unit surface.

Finally, the temperature of transition was equal to that of PNIPAM homopolymer and was not affected by adsorption of the PLL backbone. This is presumably due to the block-like nature of PNIPAM macrografts, and relative orientation of strand away from the surface that is preferably covered by the PLL backbone. One advantage of the present design of PLL-g-PNIPAM is that possible effect of ligands or co-monomers on the temperature of response can be adjusted at the stage of the PNIPAM macrograft synthesis, prior to attachment on PLL, in order to tune the temperature of response. For instance, introduction of hydrophobic (resp. hydrophilic) moieties can be used to balance ligands hydrophilicity (resp. hydrophobicity).

CONCLUSIONS

Adsorption of cationic comb-like derivatives of poly(lysine) allows facile coating and passivation (e.g. PEGylation) of glass. It was here extended to control the surface deposition and presentation of biotin (used as a model ligand), via a versatile strategy based on i) reactive parent polymer strands, that are easily modified in bulk with any amine-containing side group prior to be coupled on PLL lysine groups, ii) T-responsive PNIPAM macrografts that hide the (biotin) ligand in their collapsed form and display them at low temperature. Robust, mixed adlayers with control composition were obtained from simple minute-long bath application on glass. Control of specific binding of beads, by variation of surface composition and/or temperature, was established. Measurements by AFM of the PLL-g-PNIPAM layers showed that sharp surface transition (variation of thickness, rigidity and roughness) occurs at 32°C. PLL derivatives enable straightforward functionalization with adjustable surface density of functional, T-responsive strands by deposition of PLL-g-PNIPAMcoLigand:PLL-g-PEG mixed solutions. This functional coating is implemented with no need for specialized chemistry skills, and it enables to adjust on demand the accessibility of a ligand of interest. This is an asset for applications aiming to optimize specific binding and surface density of bioactive ligands.

.

FIGURES
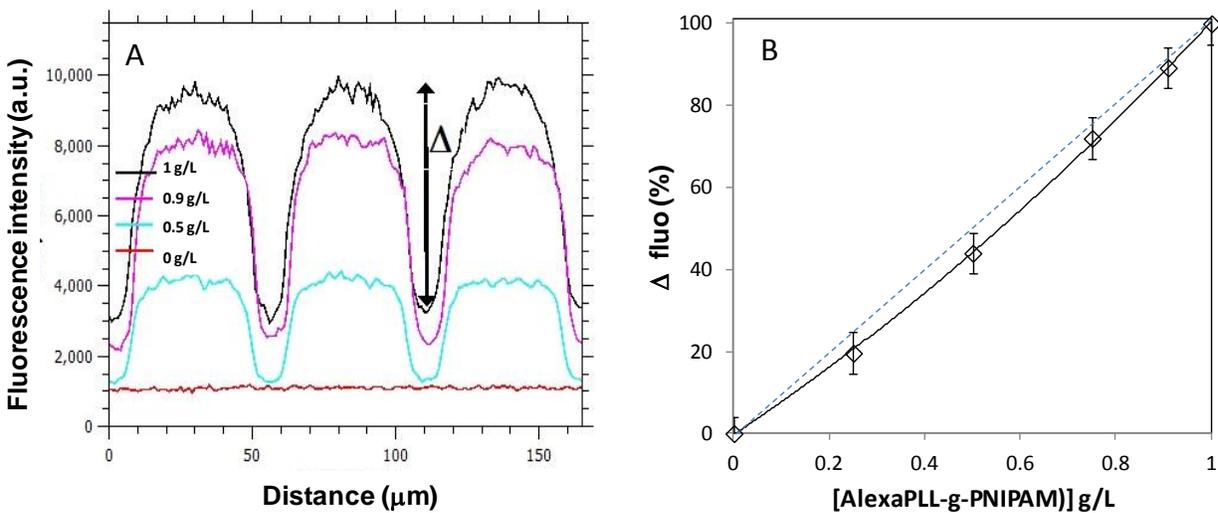
Figure 1. Fluorescence of polymer layers deposited from mixed solutions of (PLL-g-PEG):(AlexaPLL-g-PNIPAM) at 1 g/L total concentration and varying [AlexaPLL-g-PNIPAM]. (A) measurements along an axis perpendicular to UV-etched stripes, [AlexaPLL-g-PNIPAM] quoted in the figure ; (B) difference of intensities between the etched and non-etched regions ("Δ" in (A)) normalized to 100% for pure AlexaPLL-g-PNIPAM.
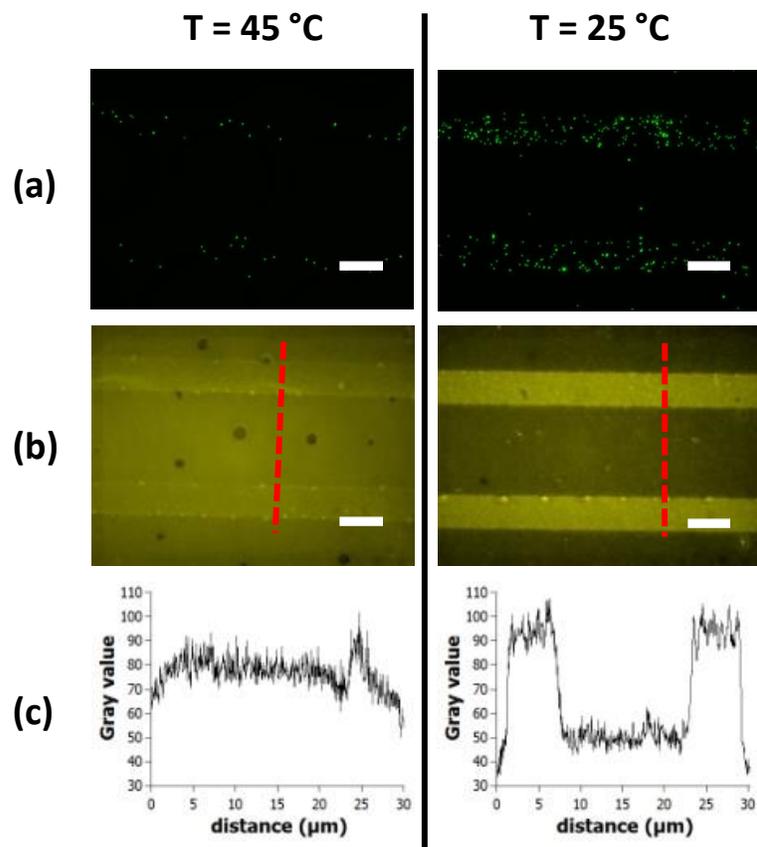
Figure 2. Epifluorescence pictures of coverslips (S_PEG/NIPAbiot) incubated with a solution of (a) fluoSphere and (b) Qdot-avidin at 45 °C or 25 °C and flushed with water. Thinner stripes were coated with PNIPAMcoBiotin chains, larger ones with PLL-g-PEG. (c) Curves show the raw fluorescence signal measured along the dashed lines (see Table S2-S4 in SI for quantitative measurements); scale bar = 6 μm.
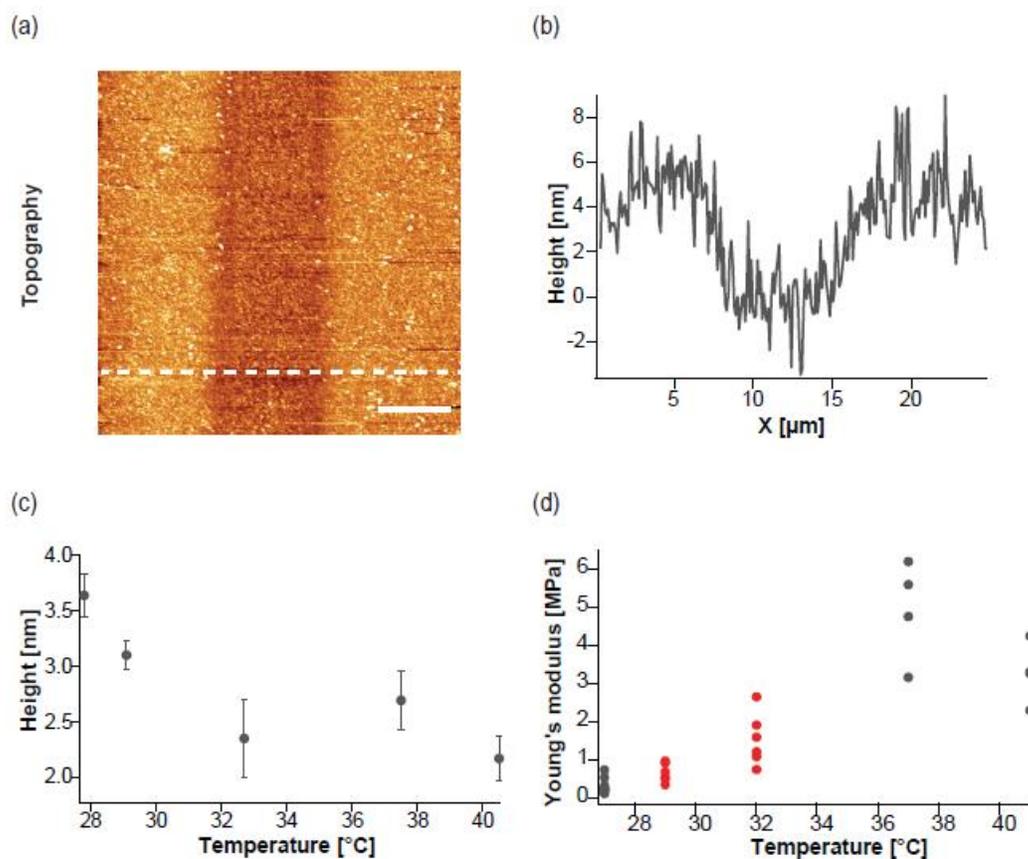
Figure 3. AFM measurements in PBS buffer on $S_{NIPA/glass}$, a coverslip coated with PLL-g-PNIPAM, and UV-etched to form stripes of bare glass alternating with polymer-coated ones (a) topographic image (full colors scale: 20nm), (b) height profile, (c) height of PLL-g-PNIPAM layer relative to the bare glass surface. Error bars represent the width of the fit of data to a gaussian distribution, (d) rigidity modulus of PLL-g-PNIPAM layer (see SI for experimental details).
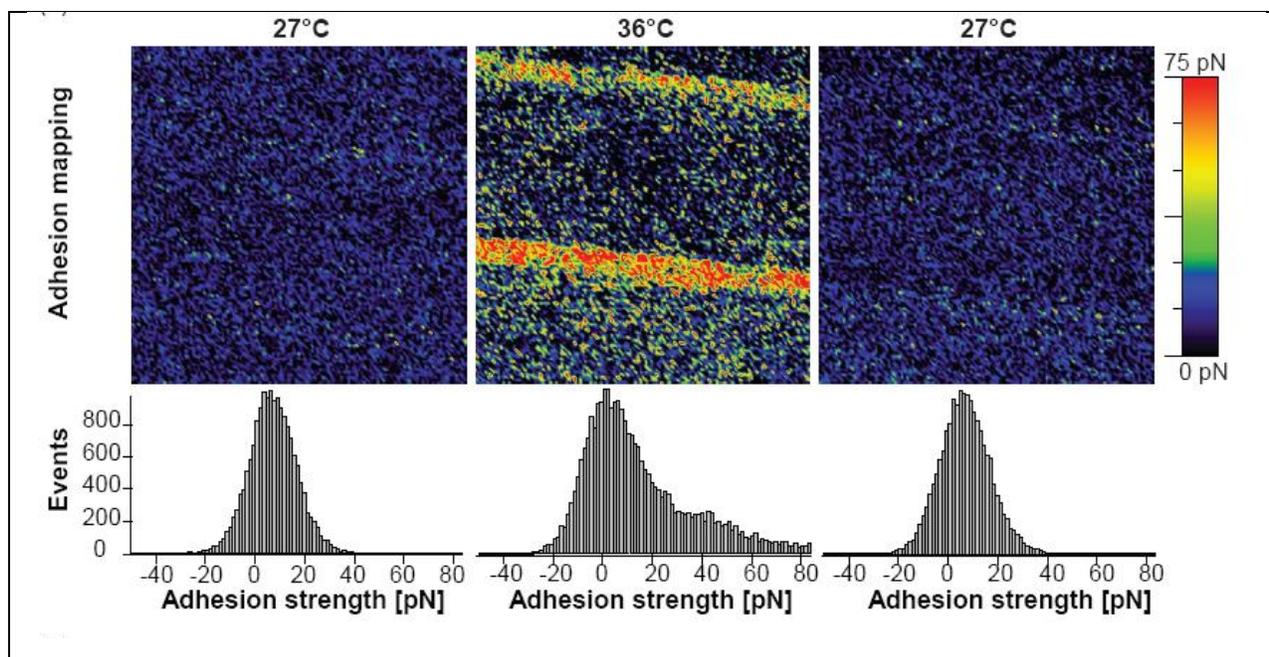
Figure 4. AFM adhesion maps and corresponding distribution of forces over the image as obtained by PeakForce QNM on S$_{PEG/NIPA}$. Imaging of the same surface area initially at 27°C (left) and heated up to 37°C (middle) then cooled down (right) in the AFM cell.
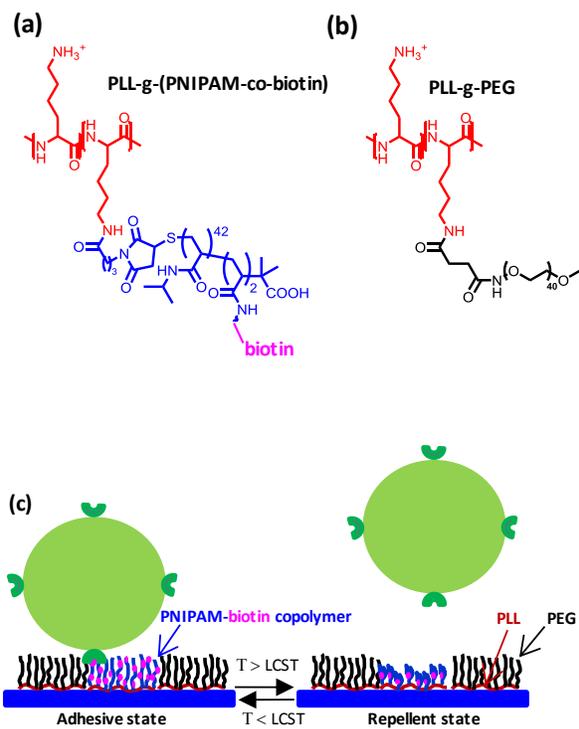
Scheme 1. Functional comb-like poly(lysine) derivatives deposited in mixed layers by adsorption on glass substrates to achieve temperature switched specific binding of particles
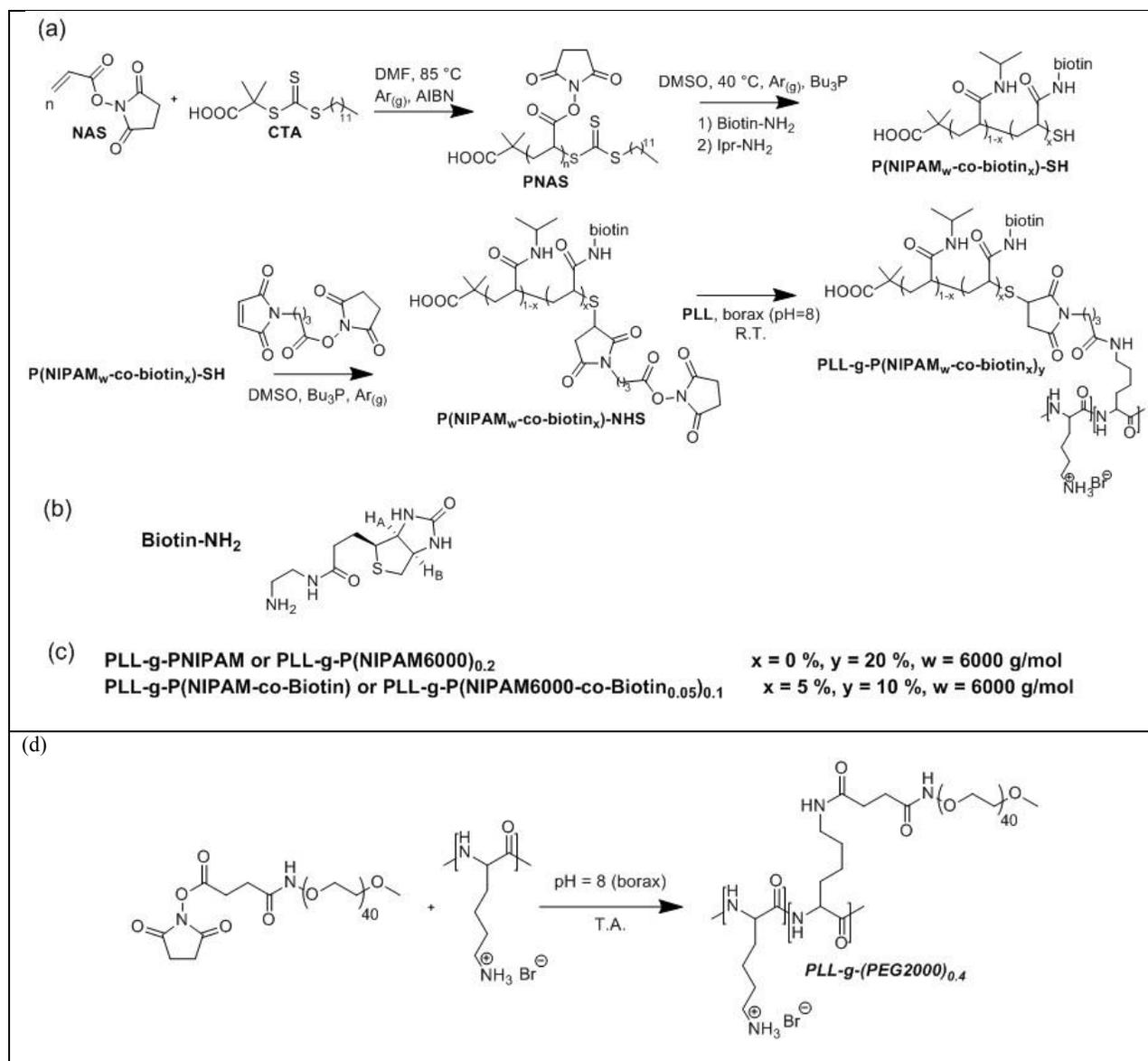
Scheme 2. Synthetic route to PLL-g-(PNIPAM-co-biotin) and (d) PLL-g-PEG
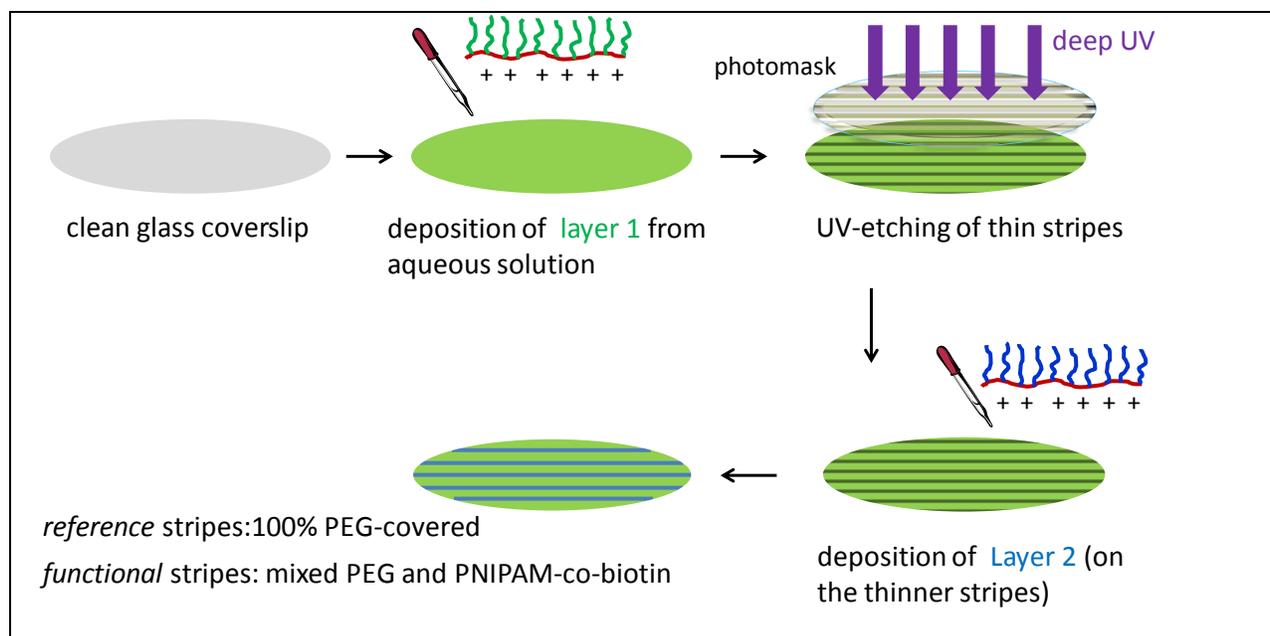
Scheme 3. Step-wise procedure by applications of PLL solutions and deep-UV etching resulting in the deposition on glass of PLL comblike derivatives along stripes coated by diverse polymer layers. Stripes covered with 100% PLL-g-PEG were used as highly repellent control regions. Larger stripes were covered either by 100% PLL-g-PEG layer ($S_{PEG/NIPAxx}$ in Table 1), or fluorescently-labelled PNIPAM (Figure 1 or $S_{NIPA/glass}$ in Table 1). Thinner ones were coated with PLL-g-PNIPAM (or PLL-g-PNIPAMcobiotin) mixed or not with PLL-g-PEG

ASSOCIATED CONTENT

Supporting Information. NMR spectrum, SEC, and data on chain growth of polyNAS, additional fluorescent images of polymer-coated coverslips, and AFM topographs are supplied as Supporting Information . This material is available free of charge via the Internet at http://pubs.acs.org.

AUTHOR INFORMATION

Corresponding Author

* Christophe.tribet@ens.fr.

Present Addresses

†

Author Contributions

The manuscript was written through contributions of all authors. All authors have given approval to the final version of the manuscript.

REFERENCES

1.   Zhai, L., Stimuli-responsive polymer films. *Chem. Soc. Rev.* **2013**, *42*, 7148-7160.

2.   Welch, M. E.; Ober, C. K., Responsive and Patterned Polymer Brushes. *J. Pol. Sci. B: Pol. Phys.* **2013**, *51* (20), 1457-1472.

3.   Jungwook, K.; Jinhwan, Y.; Hayward, R. C., Dynamic display of biomolecular patterns through an elastic creasing instability of stimuli-responsive hydrogels. *Nature Materials* **2010**, *9*, 159-164.

4.   Gibson, M. I.; O'Reilly, R. K., To aggregate, or not to aggregate? considerations in the design and application of polymeric thermally-responsive nanoparticles. *Chem Soc Rev* **2013**, *42*, 7204-7213.

5.   Krishnamoorthy, M.; Hakobyan, S.; Madeleine Ramstedt; Gautrot, J. E., Surface-Initiated Polymer Brushes in the Biomedical Field: Applications in Membrane Science, Biosensing, Cell
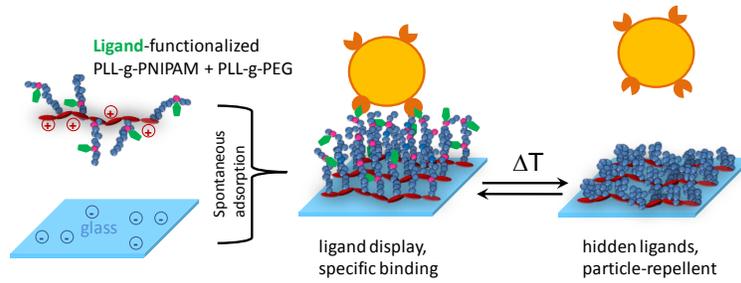
Culture, Regenerative Medicine and Antibacterial Coatings. *Chem. Rev.* **2014,** *114* (21), 10976-11026.

6.   Tang, Z.; Akiyama, Y.; Okano, T., Recent Development of Temperature-Responsive Cell Culture Surface Using Poly(N-isopropylacrylamide). *J. Pol. Sci. B: Pol. Phys.* **2014,** *52*, 917-926.

7.   Desseaux, S.; Klok, H.-A., Temperature-Controlled Masking/Unmasking of Cell-Adhesive Cues with Poly(ethylene glycol) Methacrylate Based Brushes. *Biomacromolecules* **2014,** *15*, 3859-3865.

8.   Fang, B.; Jiang, Y.; Rotello, V. M.; Nüsslein, K.; Santore, M. M., Easy Come Easy Go: Surfaces Containing Immobilized Nanoparticles or Isolated Polycation Chains Facilitate Removal of Captured Staphylococcus aureus by Retarding Bacterial Bond Maturation. *ACS Nano* **2014,** *8* (2), 1180-1190.

9.   Pan, G.; Guo, B.; Ma, Y.; Cui, W.; He, F.; Li, B.; Yang, H.; Shea, K. J., Dynamic Introduction of Cell Adhesive Factor via Reversible Multicovalent Phenylboronic Acid/cis-Diol Polymeric Complexes. *J. Am. Chem. Soc.* **2014,** *136*, 6203−6206.

10.   Lanotte, L.; Guido, S.; Misbah, C.; Peyla, P.; Bureau, L., Flow Reduction in Microchannels Coated with a Polymer Brush. *Langmuir* **2012,** *28* (38), 13758–13764.

11.   Malmstadt, N.; Yager, P.; Hoffman, A. S.; Stayton, P. S., A smart microfluidic affinity chromatography matrix composed of poly(N-isopropylacrylamide)-coated beads. *Anal. Chem.* **2003,** *75* (13), 2943-2949.

12.   Paumier, G.; Sudor, J.; Gue, A.-M.; Vinet, F.; Li, M.; Chabal, Y. J.; Esteve, A.; Djafari-Rouhani, M., Nanoscale actuation of electrokinetic flows on thermoreversible surfaces. *Electrophoresis* **2008,** *29* (6), 1245-1252.

13.   Halperin, A.; Kröger, M., Thermoresponsive Cell Culture Substrates Based on PNIPAM Brushes Functionalized with Adhesion Peptides: Theoretical Considerations of Mechanism and Design. *Langmuir* **2012,** *28*, 16623-16637.

14.   Ishida, N.; Biggs, S., Effect of Grafting Density on Phase Transition Behavior for Poly(N-isopropylacryamide) Brushes in Aqueous Solutions Studied by AFM and QCM-D. *Macromolecules* **2010,** *43* (17), 7269-7276.

15.   Choi, S.; Choi, B.-C.; Xue, C.; Leckband, D., Protein Adsorption Mechanisms Determine the Efficiency of Thermally Controlled Cell Adhesion on Poly(N-isopropyl acrylamide) Brushes. *Biomacromolecules* **2013,** *14*, 92−100.

16.   H.-P.Huang; Michel, R.; Vörös, J.; Textor, M.; Hofer, R.; Rossi, A.; Elbert, D. L.; HubbellSpencer, J. A., Poly(L-lysine)-g-poly(ethylene glycol) layers on metal oxide surfaces: surface-analytical characterization and resistance to serum and fibrinogen adsorption. *Langmuir* **2001,** *17*, 489-498.

17.   Kenausis, G. L.; Voros, J.; Elbert, D. L.; Huang, N.; Hofer, R.; Ruiz-Taylor, L.; Textor, M.; Hubbell, J. A.; Spencer, N. D., Poly(L-lysine)-g-poly(ethylene glycol) layers on metal oxide surfaces: attachment mechanism and effects of polymer architecture on resistance to protein adsorption. *J. Phys. Chem. B* **2000,** *104*, 3298-3309.

18.   van Dongen, S. F. M.; Janvore, J.; van Berkel, S. S.; Marie, E.; Piel, M.; Tribet, C., Reactive protein-repellent surfaces for the straightforward attachment of small molecules up to whole cells. *Chem. Sci.* **2012,** *3* (10), 3000-3006.

19.   van Dongen, S. F. M.; Maiuri, P.; Marie, E.; Tribet, C.; Piel, M., Triggering Cell Adhesion, Migration or Shape Change with a Dynamic Surface Coating. *Advanced Mater.* **2013,** *25* (12), 1687-1691.

20.   Thomas, D. B.; Convertine, A. J.; Myrick, L. J.; Scales, C. W.; Smith, A. E.; Lowe, A. B.; Vasilieva, Y. A.; Ayres, N.; McCormick, C. L., Kinetics and molecular weight control of the polymerization of acrylamide via RAFT. *Macromolecules* **2004,** *37* (24), 8941-8950.

21.   Qiu, X.-P.; Winnik, F. M., Synthesis of alpha,omega-dimercapto poly(N-isopropylacrylamides) by RAFT polymerization with a hydrophilic difunctional chain transfer agent. *Macromolecules* **2007,** *40* (4), 872-878.

22.   Zhu, X.; Yan, C.; Winnik, F. M.; Leckband, D., End-grafted low-molecular-weight PNIPAM does not collapse above the LCST. *Langmuir* **2007,** *23* (1), 162-169.

23.   Rico, F.; Su, C. M.; Scheuring, S., Mechanical Mapping of Single Membrane Proteins at Submolecular Resolution. *Nano Lett.* **2011,** *11*, 3983-3986.

24.   Eghiaian, F.; Rigato, A.; Scheuring, S., Structural, Mechanical and Dynamical variability of the actin cortex in living cells. *Biophys. J.* **2015,** *108* (6), 1330-1340.

25.   Yim, H.; Kent, M. S.; Mendez, S.; Lopez, G. P.; Satija, S.; Seo, Y., Effects of Grafting Density and Molecular Weight on the Temperature-Dependent Conformational Change of Poly(N-isopropylacrylamide) Grafted Chains in Water. *Macromolecules* **2006,** *39*, 3420-3426.

26.   Dimitriadis, E. K.; Horkay, F.; Maresca, J.; Kachar, B.; Chadwick, R. S., Determination of elastic moduli of thin layers of soft material using the atomic force microscope. *Biophys. J.* **2002,** *82* (5), 2798-2810

27.   Ionov, L.; Minko, S., Mixed Polymer Brushes with Locking Switching. *ACS Appl. Mater. & Interf.* **2012,** *4* (1), 483-489.

28.   Xiong, X.; Wu, Z.; Yu, Q.; Xue, L.; Du, J.; Chen, H., Consecutive Free-Radical- and Visible-Light-Induced Polymerization : Reversible Bacterial Adhesion on Mixed Poly(dimethylaminoethyl methacrylate)/Poly(acrylamidophenyl boronic acid) Brush Surfaces. *Langmuir* **2015,** *31*, 12054−12060.

29.   Zhao, B.; Zhu, L., Nanoscale phase separation in mixed poly(tert-butyl acrylate)/polystyrene brushes on silica nanoparticles under equilibrium melt conditions. *J. Am. Chem. Soc.* **2006,** *128* (14), 4574-4575.

30.   Calabrese, D.; Ditter, D.; Liedel, C.; Blumfield, A.; Zentel, R.; Ober, C. K., Design, Synthesis, and Use of Y‑Shaped ATRP/NMP Surface Tethered Initiator. *ACS MacoLetters* **2015,** (4), 606-610.

31.   Li, W. K.; Bao, C. H.; Wright, R. A. E.; Zhao, B., Synthesis of mixed poly(epsilon-caprolactone)/polystyrene brushes from Y-initiator-functionalized silica particles by surface-initiated ring-opening polymerization and nitroxide-mediated radical polymerization. *RSC Advances* **2014,** *4* (36), 18772-18781.

32.   Bao, C. H.; Tang, S. D.; Horton, J. M.; Jiang, X. M.; Tang, P.; Qiu, F.; Zhu, L.; Zhao, B., Effect of Overall Grafting Density on Microphase Separation of Mixed Homopolymer Brushes Synthesized from Y-Initiator-Functionalized Silica Particles. *Macromolecules* **2012,** *45* (19), 8027-8036.

33.   Jiang, X. M.; Zhao, B.; Zhong, G. J.; Jin, N. X.; Horton, J. M.; Zhu, L.; Hafner, R. S.; Lodge, T. P., Microphase Separation of High Grafting Density Asymmetric Mixed Homopolymer Brushes on Silica Particles. *Macromolecules* **2010,** *43* (19), 8209-8217.

34.   Xiong, D. A.; Liu, G. J.; Duncan, E. J. S., Simultaneous Coating of Silica Particles by Two Diblock Copolymers. *ACS Appl. Mater. & Interf.* **2012,** *4* (5), 2445-2454.

35.   Louguet, S.; Rousseau, B.; Epherre, R.; Guidolin, N.; Goglio, G.; Mornet, S.; Duguet, E.; Lecommandoux, S.; Schatz, C., Thermoresponsive polymer brush-functionalized magnetic manganite nanoparticles for remotely triggered drug release. *Pol. Chem.* **2012,** *3* (6), 1408-1417.

36.   Rudov, A. A.; Potemkin, II, Surface micelles obtained by selective adsorption of AB and AC diblock copolymers. *Soft Matter* **2013,** *9* (3), 896-903.

37.   Malinge, J.; Mousseau, F.; Zanchi, D.; Brun, G.; Tribet, C.; Marie, E., Tailored stimuli-responsive interaction between particles adjusted by straightforward adsorption of mixed layers of Poly(lysine)-g-PEG and Poly(lysine)-g-PNIPAM on anionic beads. *J. Coll. Interf. Sci.* **2016,** *461*, 50-55.

38.   Zareie, H. M.; Boyer, C.; Bulmus, V.; Nateghi, E.; Davis, T. P., Temperature-responsive self-assembled monolayers of oligo(ethylene glycol): Control of biomolecular recognition. *ACS Nano* **2008,** *2* (4), 757-765.

39.   Nash, M. E.; Healy, D.; Carroll, W. M.; Elvira, C.; Rochev, Y. A., Cell and cell sheet recovery from pNIPAm coatings; motivation and history to present day approaches. *J. Mater. Chem.* **2012,** *22*, 19376-19389.

40.   Akkilic, N.; Leermakers, F. A. M.; de Vos, W. M., Responsive polymer brushes for controlled nanoparticle exposure. *Nanoscale* **2015,** *7*, 17871–17878.

41.   Delcroix, M. F.; Huet, G. L.; Conard, T.; Demoustier-Champagne, S.; Du Prez, F.; Landoulsi, J.; Dupont-Gillain, C. C., Design of Mixed PEO/PAA Brushes with Switchable Properties Toward Protein Adsorption. *Biomacromolecules* **2013,** *14* (215-225).

42.   Mastrotto, F.; Caliceti, P.; Amendola, V.; Bersani, S.; Magnusson, J. P.; Meneghetti, M.; Mantovani, G.; Alexander, C.; Salmaso, S., Polymer control of ligand display on gold nanoparticles for multimodal switchable cell targeting. *Chem. Commun.* **2011,** *47* (35), 9846-9848.
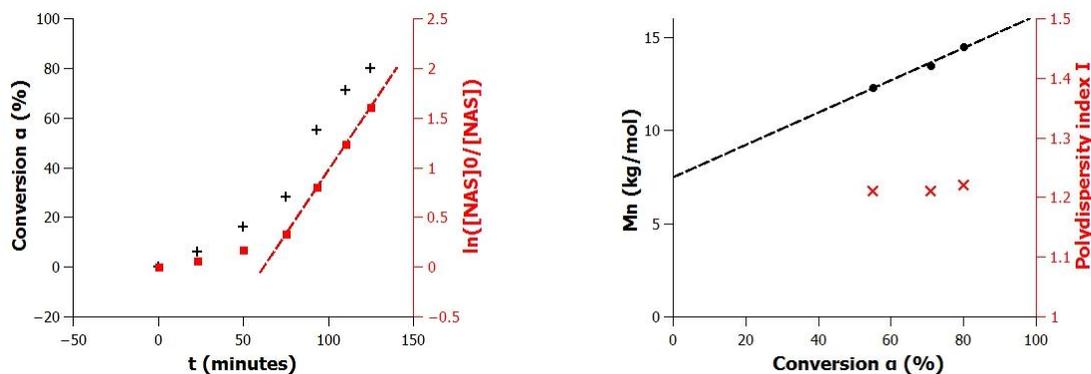
Table of Contents artwork

Ligand-functionalized PLL-g-PNIPAM + PLL-g-PEG

glass

Spontaneous adsorption

ΔT

ligand display, specific binding

hidden ligands, particle-repellent

Electronic Supplementary Information

Contents

1. Characterisation of polymer chains

Figure S1. characteristic features of RAFT polymerization of NAS in DMF at 85 °C ([NAS]$_0$ = 3 mol/L; [NAS]$_0$/[CTA]$_0$ = 50 ; [CTA]$_0$/[AIBN]$_0$ = 10) : (a) kinetical monitoring by ^{1}H-NMR, (b) Mn and I versus conversion.

Polymerization was stopped by freezing the flask in liquid nitrogen after 2h reaction, i.e. at 80% conversion. The polymer was precipitated twice in dried diethylether. After drying under vacuum, the product was obtained as a yellow powder (1.54 g, 51 %). The dispersity of chain length was estimated by SEC. Mn was calculated from ^{1}H-NMR spectrum.

δ (RMN-^{1}H, DMSO) : 0.85 (t, J = 6.4 Hz, 3H), 1.24 (m, 20H), 1.71-2.40 (s, 100H), 2.74-2.87 (s, 186H), 2.98-3.25 (s, 55H), 10.55 (s, 1H) ; M$_n$ (NMR)= 8.8 kg.mol^{-1} , Ip (SEC)= 1.2
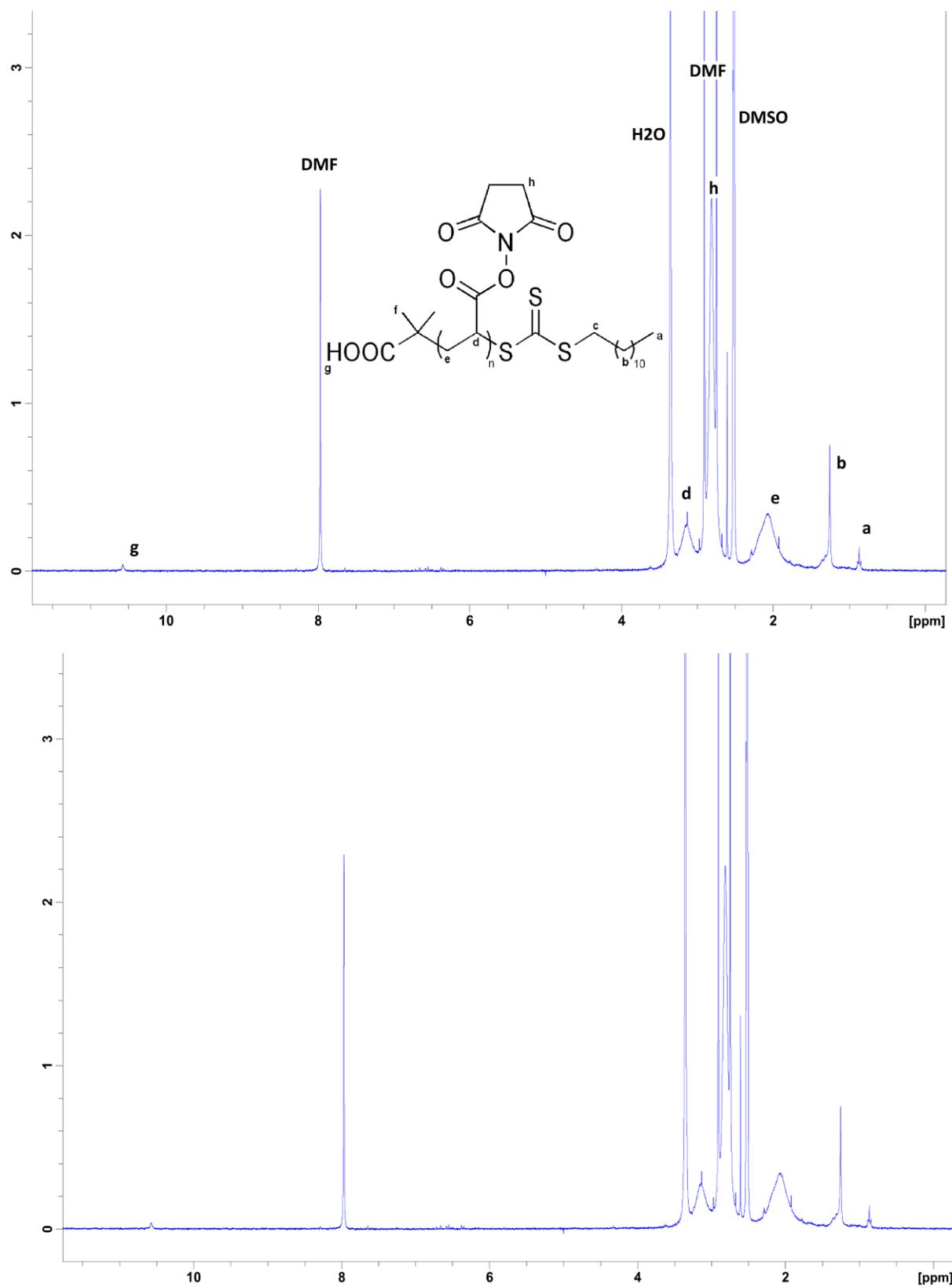
Figure S2. ^{1}H-NMR spectrum of the polyNAS in DMSO after two precipitations in dried diethylether.

Time of reaction	Conversion $\alpha^{(a)}$	DP$_n$			M$_n$ (kDa)			I$^{(d)}$
		Theoretical$^{(b)}$	NMR$^{(a)}$	SEC$^{(c)}$	Theoretical$^{(c)}$	NMR$^{(c)}$	SEC$^{(d)}$	
2 H 05	80 %	40	50	83	7.1	8.8	14.5	1.2

Table S1. Characteristic features of PNAS obtained by RAFT polymerization (2h in DMF at 85 °C; $[NAS]_0 = 3$ mol/L; $[NAS]_0/[CTA]_0 = 50$; $[CTA]_0/[AIBN]_0 = 10$) and purified by two precipitations in dried diethylether. (a) Evaluated by ^{1}H-NMR in DMSO-d6, (b) calculated from DP$_{n\ theoretical} = \alpha \times \frac{[NAS]_0}{[CTA]_0}$, (c) calculated from M$_n$ = DP$_n$ $\times$ M$_{NAS}$ + M$_{CTA}$, (d) evaluated by simple-detection SEC in DMF (polystyrene standards)
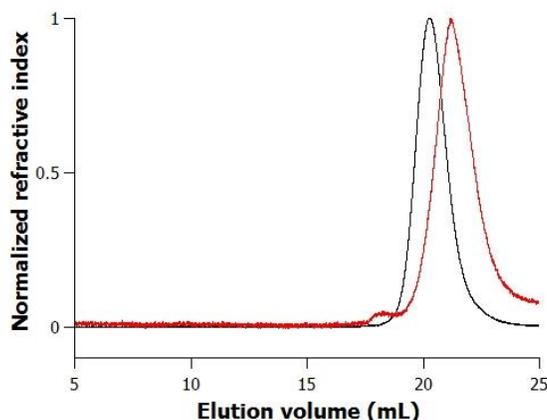
Figure S3. SEC Chromatograms of purified PNAS in DMF (black), and the macrograft derivative under the form of thiol-terminated PNIPAM (red). Elution volumes > 25 mL correspond to the elution of small molecules (Mn < 1000 g/mol); polymer chains were eluted as a single peak in the window 18mL - 24mL.

2. Surface coating

A

B
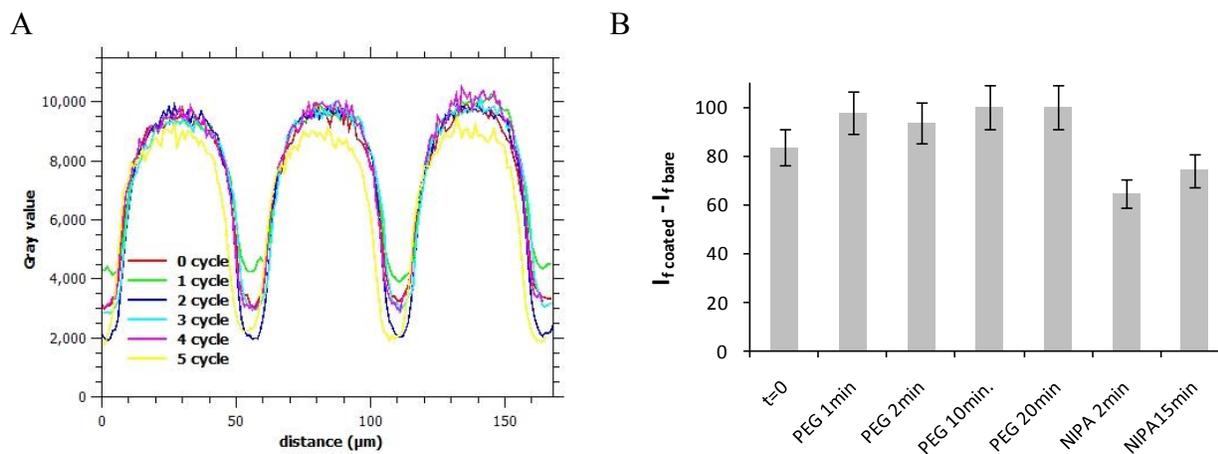
Figure S4. Fluorescence of AlexaPLL-g-PNIPAM-coated, and UV-etched, coverslips (alternative thin bare glass stripes and larger AlexaPLL-g-PNIPAM-coated ones) as evaluated by epifluorescence microscopy along a line orthogonal to the stripes. (A) coverslip subjected to 0 to 5 successive cycles of temperature sweep (in one cycle, the coverslip was immersed in water at 45 °C for 2-3 min., then in water at 25 °C); (B) after application of a solution of PLL-g-PEG (1 g/L) for increasing incubation times (I$_{f\ coated}$ - I$_{f\ bare}$ is the difference between fluorescence intensities of the large stripes and thin ones, normalized by the maximum value measured in the data set). Upon exposure to PLL-g-PEG, the bare stripes were coated with PLL-g-PEG. They were rinsed with water, and eventually incubated in an aqueous solution of 1g/L AlexaPLL-g-PNIPAM for 2 minutes (NIPA 2min) and 15 minutes (NIPA 15 min).

# 3. Blank experiments showing the (weak) non-specific adsorption of beads.
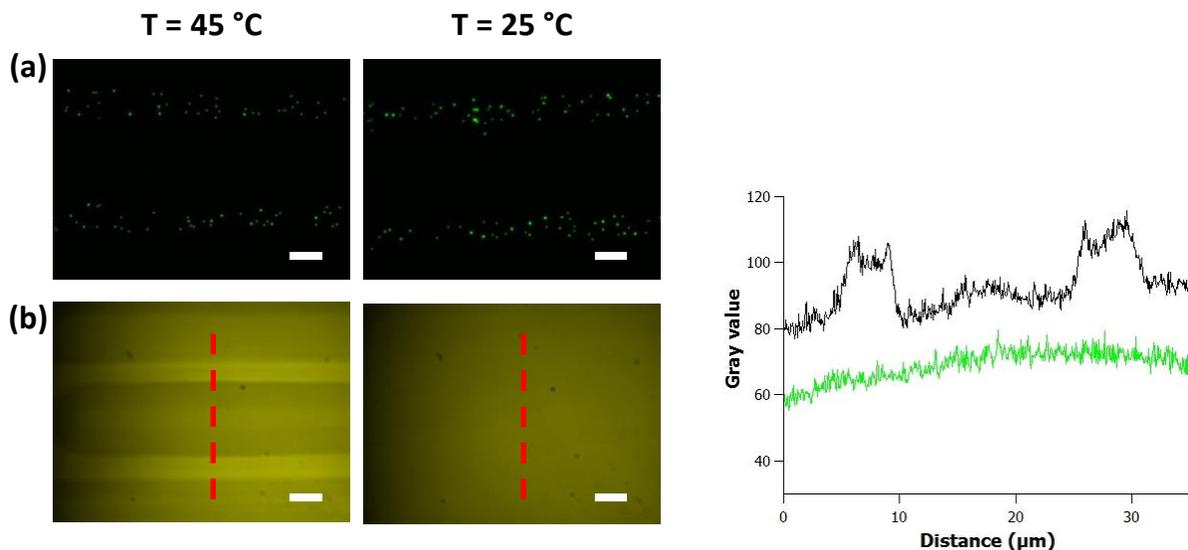
Figure S5. Epifluorescence pictures obtained from $S_{\text{NIPAM:PEG}}$ coverslip (alternative stripes of 100% PLL-g-PEG without biotin, and 100% PLL-g-PNIPAM) incubated with a solution of (a) fluoSphere and (b) Qdot-avidin at 45 °C or 25 °C (scale bar = 6 μm), (c) profile of the fluorescent intensity along the red line in (b) chosen to display a profile having the highest contrast within the images collected in these conditions; green = 25°C, black=45°C.
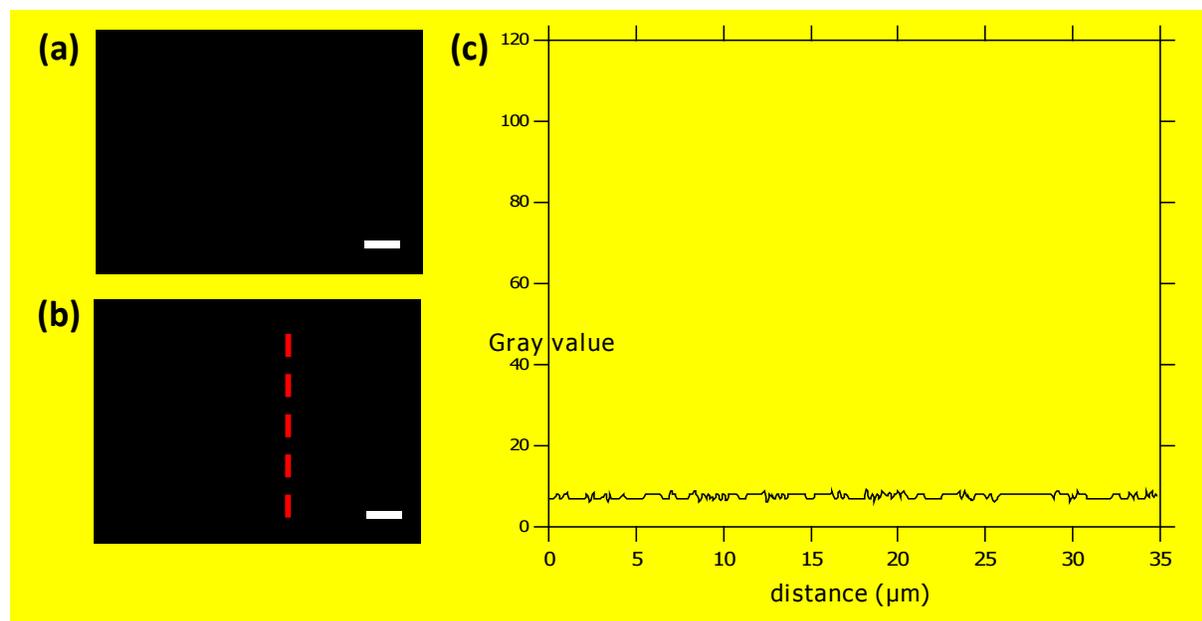
Figure S6. Epifluorescence pictures obtained on bare glass coverslip after incubation (a) with fluoSphere, and (b) with Qdot-avidin and water rinse ; (c) profile of the fluorescent intensity along the red line in (b) (scale bar = 6 μm)

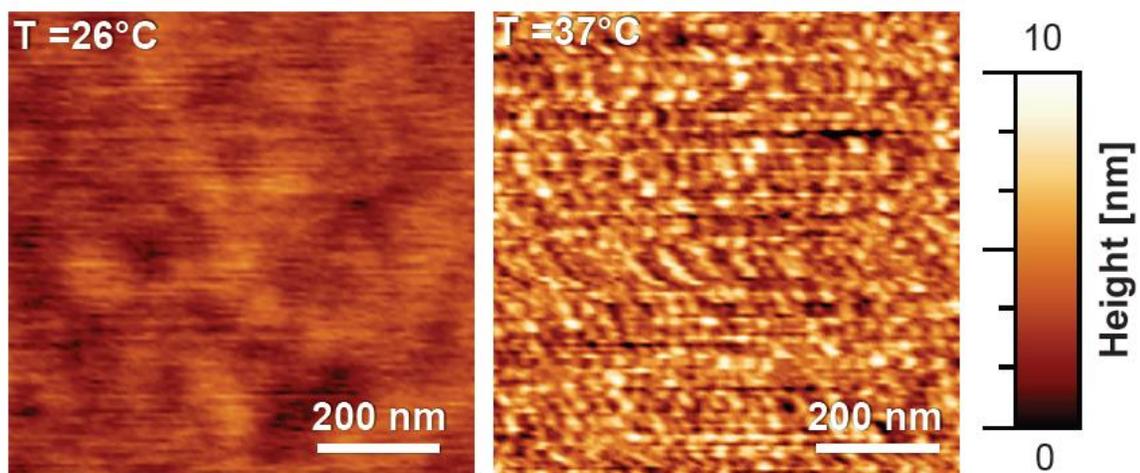| T (°C)	$S_{PEG/NIPAbiot}$	$S_{PEG/NIPAbiot:PEG\ 3:1}$	$S_{PEG/NIPA}$
25	50	77	60
45	70	90	85
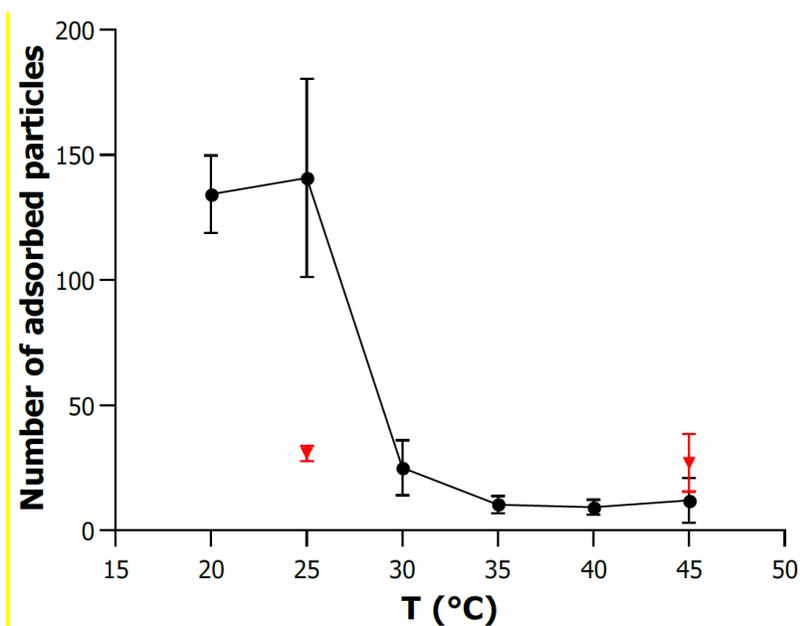
Figure S7. Number of FluoSpheres counted on a stripe coated with 100% PLL-g-NIPAMco-biotin (circles, $S_{PEG/NIPAbiot}$, total surface of 351 μm^2) incubated with Neutravidin-coated FluoSpheres at increasing temperature. Red triangles are controls on PLL-g-PNIPAM stripe (in $S_{PEG/NIPA}$ sample).
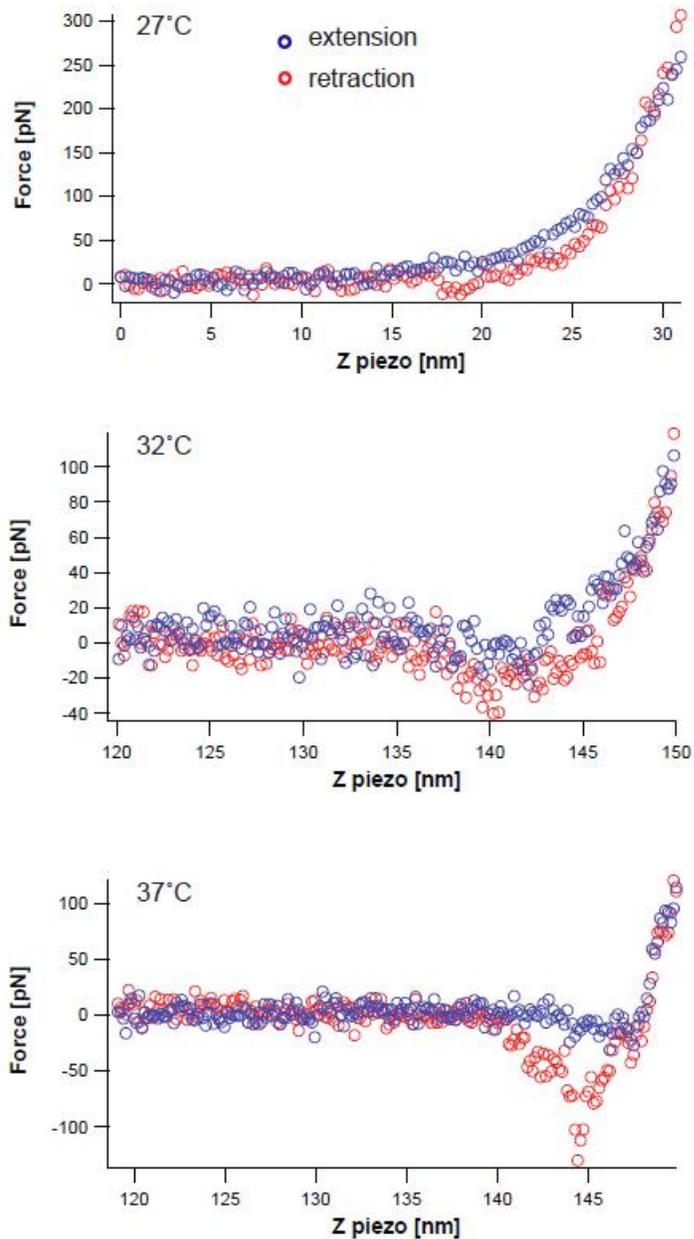
4. AFM

Figure S8. PF-QNM AFM topographs (full color scale : 10nm) in PBS Buffer.
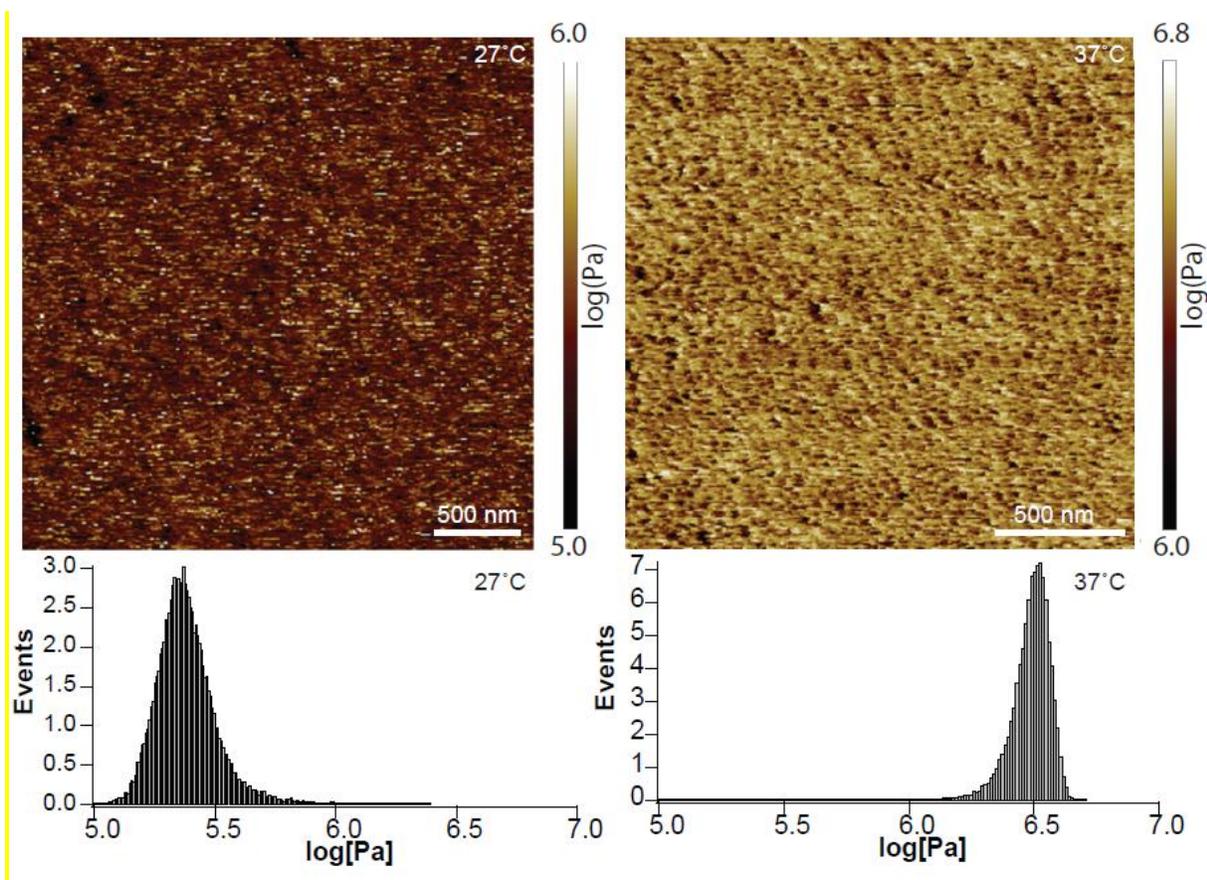
Figure S9. PeakForce nanomechanical maps obtained on the PNIPAM layers below and above phase transition

References.

1.   D. B. Thomas, A. J. Convertine, L. J. Myrick, C. W. Scales, A. E. Smith, A. B. Lowe, Y. A. Vasilieva, N. Ayres and C. L. McCormick, *Macromolecules*, 2004, **37**, 8941-8950.

2.   X.-P. Qiu and F. M. Winnik, *Macromolecules*, 2007, **40**, 872-878.
3.   E. K. Dimitriadis, F. Horkay, J. Maresca, B. Kachar and R. S. Chadwick, *Biophysical Journal*, 2002, **82**, 2798-2810.
4.   L. Picas, F. Rico and S. Scheuring, *Biophysical Journal*, 2012, **102**, L1-L3.